Sustainable Horizons 11 (2024) 100098

Contents lists available at ScienceDirect

Sustainable Horizons

journal homepage: www.elsevier.com/locate/horiz

Original Research Articles

Assessment and prediction of significant wave height using hybrid CNN-BiLSTM deep learning model for sustainable wave energy in Australia

Nawin Raj [a,*], Reema Prakash [b]

[a] School of Mathematics, Physics and Computing, Springfield Campus, University of Southern Queensland, Toowoomba, QLD 4300, Australia
[b] School of Agriculture, Geography, Environment, Ocean and Natural Sciences, The University of the South Pacific, Suva, Fiji

A R T I C L E I N F O

Keywords:
Multivariate Variational Mode Decomposition (MVMD)
Convolutional Neural Network (CNN)
Bidirectional LSTM (BiLSTM)
Significant Wave Height (H_s)
Intrinsic Mode Functions (IMFs)

A B S T R A C T

Wave energy is regarded as one of the powerful renewable energy sources and depends on the assessment of significant wave height (H_s) for feasibility. Hence, this study explores the potential of wave energy by assessing and predicting H_s for two study sites in Queensland (Emu Park and Townsville), Australia. Assessment and prediction of H_s is extremely important for reliable planning, cost management and implementation of wave energy projects. The study utilized oceanic datasets based on wave measurements obtained from buoys along coastal regions of Queensland that are transmitted to nearby receiver stations. The parameters of the datasets include maximum wave height, zero up crossing wave period, peak energy wave period and sea surface temperature to accurately predict Hs. A new hybrid Convolutional Neural Network (CNN) and Bidirectional Long Short Term (BiLSTM) deep learning model with Multivariate Variational Mode Decomposition (MVMD) is developed which is benchmarked by Multi-Layer Perceptron (MLP), Random Forest (RF) and Categorical Boosting (CatBoost) to compare the performance. All models attain relatively high-performance results. The MVMD-CNN-BiLSTM attains slightly better performance values for both study sites among all developed models with highest correlation values of 0.9957 and 0.9986 for Emu Park and Townsville, respectively. Other performance evaluation metrics were also higher for MVMD-CNN-BiLSTM with lowest error values in comparison to the benchmark models. The annual mean of H_s is also computed to compare and obtain an insight with a linear projection. There is a greater ocean wave energy potential for Emu Park for a 10-year period with a projected mean H_s of 0.865 m in comparison to Townsville where the projected mean was of 0.665 m.

1. Introduction

Generation of energy from fossil fuels is a major contributor of carbon emissions causing global warming and climate change. Reduction of greenhouse gas emissions from energy production requires more reliance on renewable energy and ocean energy represent a clean source with zero carbon emissions. Wave energy is one of the most powerful renewable energy source (López et al., 2013; Veerabhadrappa et al., 2022) derived from ocean waves. Substantial amount of kinetic energy present in the rigorous vertical movement of ocean surface waves is converted into electricity by using wave energy convertors. Significant Wave Height (H_s) is an average measurement of the largest one third of the waves (Ribal and Young, 2019; Vanem, 2016) that occur over a given period of time. H_s is an important parameter of ocean waves and is an important factor for the wave energy and wave power generation. A wave monitoring buoy is used to measure H_s and other associated parameters. It provides a standardized statistic for the characteristic height of the random ocean waves offering valuable information about the waves and its dynamics on the coastal and offshore structures. The site selection of a wave energy farm and the performance of wave energy convertors and their economic feasibility is strongly influenced by the inter-annual and seasonal changes of the wave climate (Caloiero et al., 2022; Guillou and Chapalain, 2020). Advance knowledge of H_s and it's forecasting is therefore crucial for sustainable management of wave energy (Chen et al., 2023).

The prediction of wave height has been a significant topic of research in the past utilizing data based and numerical methods. Many factors affect wave energy forecast as stated in Zheng and Song (2021) which includes wave power, significant wave height and wave period. A number of studies have used data driven models for prediction of H_s which include models such as neural networks technique (Deo et al., 2002) numerical wave model (Jain et al., 2011), fuzzy K-nearest

* Corresponding author.
E-mail address: nawin.raj@usq.edu.au (N. Raj).

https://doi.org/10.1016/j.horiz.2024.100098
Received 27 October 2023; Received in revised form 26 January 2024; Accepted 15 February 2024
Available online 29 February 2024

Table 1
Details of study site location and description.

Location area	Geographical location
Emu Park	23°15′25″S, 150°49′35″E
Townsville	19° 15′ 27.44″ S, 146° 49′ 4.363″ E

neighbor (FKNN) model and hybrid ensemble empirical mode decomposition (EEMD)–bidirectional long short-term memory (BiLSTM) model (Raj and Brown, 2021). A numerical forecasting experiment of the South China Sea wave energy was done by Zheng et al. (2016) using WAVEWATCH-III wave model.

Wave signals contain many patterns and relationships in its spectrum hence for more efficient prediction of H_s with data driven modelling, use of data decomposition technique is advantageous. A study by Yang et al. (2021) used Seasonal-Trend Decomposition (STL) procedure based on loess and one-dimensional Convolutional Neural Network (CNN) with Positional Encoding (PE) to accurately forecast significant wave height. Data decomposition is a useful technique in data modelling and helps to identify and separate useful features into its respective components. Past studies have also used various decomposition techniques to separate data into its IMFs before predictions using artificial intelligence (AI). Wavelet decomposed neural network was used to forecast H_s in Indian and Pacific ocean (Deka and Prahlada, 2012). Studies in the Atlantic ocean (Chen et al., 2023; Zhou et al., 2021), utilized Empirical Mode Decomposition (EMD) with Long Short Term Memory (LSTM) to forecast $H_{s.}$ An enhanced version of EMD in Ensemble Empirical Mode Decomposition (EEMD) was explored in (Raj and Brown, 2021; Song et al., 2023) with deep learning (DL) model for H_s forecasting. Waves can be predicted more accurately with the combination of EMD and machine learning than models using machine learning alone (Feng et al., 2022). Complete Ensemble Empirical Mode Decomposition with Adaptive Noise (CEEMDAN) is an improved version of EEMD and was combined with deep learning in (Raj et al., 2022) for sea level rise and in (Zhao et al., 2023) for H_s prediction. All decomposition techniques mentioned above contributed to improved predictions for DL models. With the advancement in DL architecture, hybrid DL models have acquired the ability to accurately forecast climate and environment variables in data modelling with quality data inputs. Superior accuracy of hybrid DL models when compared to standalone AI models for forecasting have been reported in Ahmed et al. (2022), Ahmed et al. (2021a), Ahmed et al. (2021b), Sharma et al. (2022) and Yang et al. (2021).

Research on hybrid DL models for accurate forecasting ocean wave energy is expanding and this study contributes a new accurate and reliable H_s forecasting model. The study aims to decompose the wave data into its intrinsic mode functions (IMFs) *via* a decomposition technique known as the Multivariate Variational Mode Decomposition (MVMD). Although many studies have focused on H_s forecasting, no study has utilized a MVMD decomposition with hybrid DL model for Australian based study sites. Being located at the right coastline orientation, Australia has the potential to generate one-third of its energy demand through wave energy (Wimalaratna et al., 2022). The total amount of energy on the Australian shelf is largest for Western Australia and Queensland is ranked second for this (Hughes and Heap, 2010). Being amongst the richest renewable countries, Australia has an extensive capacity for wave energy and the Queensland State government has invested in numerous renewable energy projects together with wave energy (Karbasi et al., 2022). Emu Park and Townsville in Queensland are two coastal stations that represent the diverse oceanic and geophysical environments and predictions of H_s for these two sites are essential for obtaining sustainable wave energy. This study proposes a new prediction model which combines MVMD data decomposition technique with a hybrid Convolutional Neural Network (CNN) and Bidirectional Long Short-Term Memory (BiLSTM) network for Hs prediction for Emu Park and Townsville that are two potential Australian wave energy generation sites.

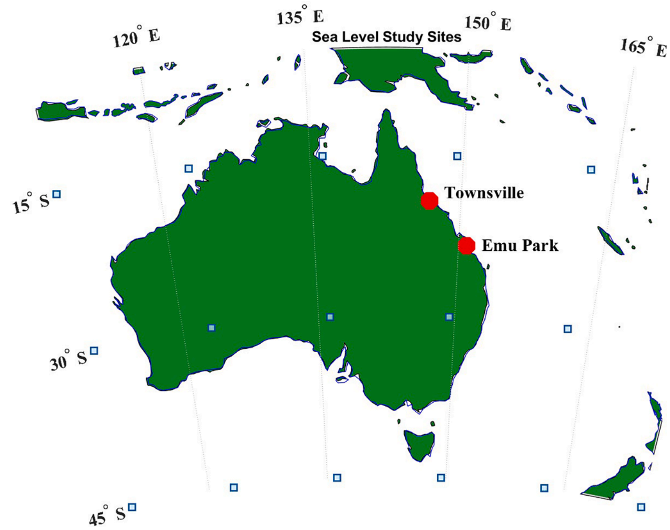

Fig. 1. Study site map of Australia showing the geographical location of Emu Park and Townsville.

Table 2
Oceanic parameters utilized for modeling in the study.

Input wave features	Description
Hmax	Maximum Wave Height
Tz	Zero up crossing wave period
Tp	Peak energy wave period
SST	Sea surface temperature
(t−1) (t−2) (t−3) (t−4) (t−5)	H_s Lags
M1, M2, M3, M4, M5, M6	Intrinsic Mode Functions (IMFs)

Table 3
ADF and KPSS analysis results for stationarity test.

ADF Statistic: −21.59	KPSS Statistic: 0.38
p-value: 0.000000	*p*-value: 0.08
Number of lags Used: 74	Number of lags Used: 74
Critical values:	Critical values:
10 %: −2.56	10 %: 0.347
5 %: −2.86	5 %: 0.463
1 %: −3.43	1 %: 0.739
ADF Result: The Series is Stationary	KPSS Result: The Series is Stationary

2. Method and data

2.1. Study area and dataset

Two coastal stations in Queensland; Emu Park and Townsville (Table 1 and Fig. 1) were chosen for wave height prediction. Data on the oceanic parameters (Table 2) for the two locations were utilized for this study.

The dataset in this study was obtained from Queensland Open Portal (Coastal Data System – Near real time storm tide data - Dataset - Open Data Portal | Queensland Government accessed on 10 August 2022). The wave parameters are electronically processed by floating buoys and remotely transmitted to a nearby station as a radio signal. The receiver is connected to a computer that stores and processes the information in near real time. The buoys are equipment with internal memory back up in cases of power loss during natural disasters such as cyclones ensuring no data is lost. Table 2 shows the oceanic parameters obtained *via* Queensland Open Portal site for H_s forecasting in this study.

	Hmax	Tz	Tp	SST	t−5	t−4	t−3	t−2	t−1	M1	M2	M3	M4	M5	M6	Hs
Hmax	1.00															
Tz	0.52	1.00														
Tp	−0.05	0.48	1.00													
SST	0.16	0.05	−0.03	1.00												
t−5	0.98	0.53	−0.04	0.16	1.00											
t−4	0.97	0.53	−0.04	0.16	0.99	1.00										
t−3	0.96	0.52	−0.04	0.17	0.99	0.99	1.00									
t−2	0.96	0.52	−0.04	0.17	0.98	0.99	0.99	1.00								
t−1	0.95	0.52	−0.04	0.17	0.97	0.98	0.99	0.99	1.00							
M1	0.82	0.55	0.05	0.24	0.84	0.84	0.84	0.84	0.84	1.00						
M2	0.65	0.28	−0.10	−0.02	0.66	0.66	0.66	0.66	0.65	0.23	1.00					
M3	0.26	0.06	−0.08	−0.01	0.26	0.25	0.24	0.23	0.22	0.03	0.08	1.00				
M4	0.15	−0.03	−0.07	0.00	0.15	0.13	0.11	0.09	0.06	0.01	0.02	0.10	1.00			
M5	0.08	0.03	−0.02	0.00	0.07	0.05	0.02	−0.01	−0.03	0.00	0.01	0.03	0.09	1.00		
M6	0.04	0.03	0.00	0.00	−0.01	−0.02	0.02	0.01	−0.02	0.00	0.00	0.00	0.00	0.01	1.00	
Hs	0.98	0.54	0.00	0.16	0.99	0.99	0.98	0.97	0.97	0.84	0.66	0.26	0.15	0.08	0.04	1.00

Fig. 2. The correlation matrix for H_s with all input variables.

Table 4
Data partition for the period 2014–2021 into training, validation, and testing.

Partition	Training	Validation	Testing
Oceanic Dataset	January 2014 –October 2018	November 2018 – June 2019	July 2020 –December 2021

Table 5
Symbols used in Eqs. (3)–(10).

	Observed Data
MDO	*Mean Observed Data*
DS_i	*Simulated Data*
MDS	*Mean Simulated Data*

2.2. Stationarity test

One of the important assumptions of time series dataset modeling is based on its stationarity. However, it cannot be always assumed that the timeseries dataset is stationary and must be conformed through statistical testing. Without stationarity, the analysis cannot be used to do reliable forecasting (Manuca and Savit, 1996; Nason, 2006). Table 3 shows the results of two stationarity tests, the Augmented Dickey Fuller (ADF) (Lopez, 1997) and Kwiatkowski–Phillips–Schmidt–Shin KPSS) (Kwiatkowski et al., 1992) tests performed on Emu Park dataset. Similar results were also obtained for Townsville. The ADF tests for unit root is presented in the data as the null hypothesis (Raj and Brown, 2021). A negative value greater than the critical value rejects the null hypothesis.

2.3. Data partition and correlation

The dataset parameters were checked for correlation to determine how H_s was related to all input variables as shown in Fig. 2. It also includes 5 lags of H_s and 6 IMFs for data modeling. Table 4 below shows the data partition for the dataset into 60 % into training, 10 % validation and 30 % into testing (Table 5).

2.4. Data partition and correlation

Data normalization is an important step for data modeling in ma-

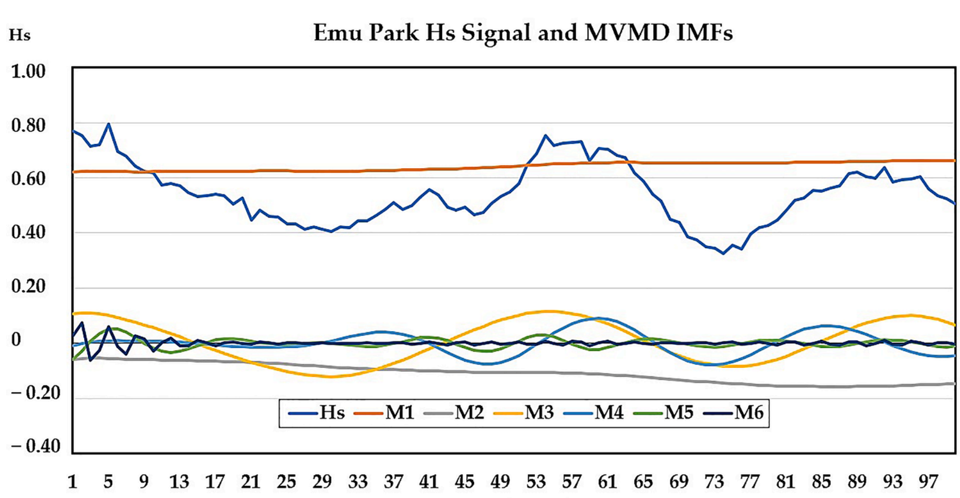

Fig. 3. H_s data decomposition into its IMFs.

```
Model: "sequential"
_________________________________________________________________
 Layer (type)                Output Shape              Param #
=================================================================
 conv1d (Conv1D)             (None, 8, 32)             96

 bidirectional (Bidirectiona  (None, 8, 20)            8480
 l)

 bidirectional_1 (Bidirectio  (None, 8, 20)            6560
 nal)

 flatten (Flatten)           (None, 160)               0

 dense (Dense)               (None, 64)                10304

 dense_1 (Dense)             (None, 1)                 65

=================================================================
Total params: 25,505
Trainable params: 25,505
Non-trainable params: 0
_________________________________________________________________
```

Fig. 4. This is a snapshot of the CNN-BiLSTM modeling architecture which shows the layers of the neural network and its hierarchy.

chine learning as it standardizes the data and improves model performance (Brink et al., 2016). The dataset used in this study was normalized using Eq. (3) and then denormalized by Eq. (4) after modeling.

$$x_n = \frac{x_{\text{raw}} - x_{\min}}{x_{\max} - x_{\min}} \tag{1}$$

$$x_{\text{raw}} = x_n(x_{\max} - x_{\min}) + x_{\min} \tag{2}$$

2.5. Data decomposition using Multivariate Variational Mode Decomposition (MVMD)

Multivariate Variational Mode Decomposition (MVMD) is an extension of Multivariate Variational Mode Decomposition (VMD). It uses a model based on multivariate modulated oscillations on the common frequency components on the input data (ur Rehman and Aftab, 2019). A collective band of limited modes that contain inherent multivariate oscillations are extracted from the data (ur Rehman and Aftab, 2019). MVMD extracts multivariate modulated oscillations and finds the oscillations in multidimensional space whereas VMD only manages to acquire univariate oscillations in the data. Fig. 3 shows the application of the algorithm to extract IMFs from the Hs signal. The sea level signal was decomposed into its intrinsic mode functions and the number was determined based on the structure of the decomposed features. A smooth curve was an indication of successful feature as input otherwise the signal was further decomposed to reveal the hidden features and used as inputs for modelling.

2.6. AI models and data modelling

2.6.1. Benchmark models

The MLP model is a widely used AI model in the modeling and prediction of climate and environment variables. It does not make prior assumption about the data distribution and has the capability to model highly nonlinear functions (Gardner and Dorling, 1998). The MLP architecture contains a network of connected neurons of nonlinear mapping between an input and output vector (Gardner and Dorling, 1998). Random Forest (RF) is motivated by the principle on enhancement of variance gains by reduction of correlation between the quantities being averaged (Segal, 2004). It was initially presented by Breiman (2001) and is a supervised machine learning algorithm. RF has proven to have high

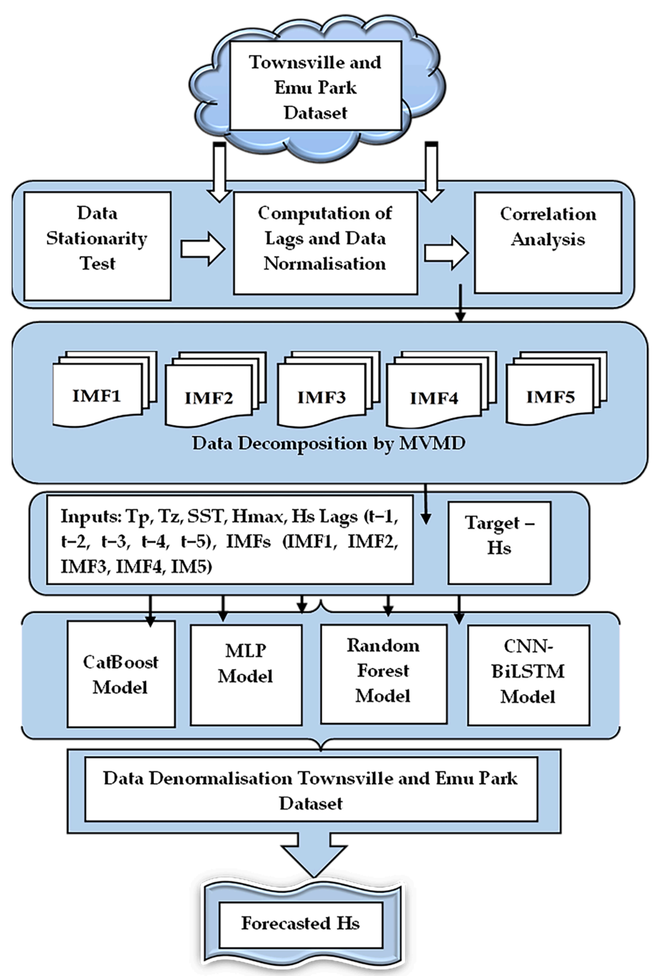

Fig. 5. Schematic representation of the overall modeling process for H_s forecasting.

Table 6
The model performance metrics for Emu Park.

Model	Correlation Coefficient (r)	Willmott's Index of agreement (d)	Nash–Sutcliffe' Coefficient (NS)	Legates and McCabes' index (LM)
MVMD-RF	0.9952	0.9938	0.9902	0.9146
MVMD-MLP	0.9951	0.9913	0.9870	0.8962
MVMD-CatBoost	0.9954	0.9942	0.9909	0.9163
MVMD-CNN-BiLSTM	0.9957	0.9946	0.9914	0.9196

robustness performance against outliers and approximate variables with nonlinear relationships (Segal, 2004). CatBoost belongs to the family of Gradient Boosted Decision Trees (GBDT's) machine learning techniques (Hancock and Khoshgoftaar, 2020). It was proposed by Prokhorenkova et al. (2018) and can be used to solve problems with heterogeneous features, complex dependencies and noisy data (Zhang et al., 2020). Performance of CatBoost was better than SVM and RF models when predicting reference evapotranspiration in humid regions in (Huang et al., 2019).

2.6.2. Objective model CNN-BiLSTM

The objective model is developed by utilizing the deep learning architectures of Convolutional Neural Network (CNN) and Bidirectional Neural Network (BiLSTM). CNN mimics the visual cortex of the human brain and uses layers of neural network (Chua and Roska, 1993). The CNN kernels and mapping structure is usually two dimensional, however this study applies one dimensional CNN where the kernels and feature structures are all one dimensional. This layer helps to extract significant features from the input dataset (Zhang et al., 2021). The input data is then passed through the two BiLSTM layers which comprises of bidirectional LSTM network. It has the capability of learning from long data sequences where the signal propagates in forward and backward direction (Aslan et al., 2021). Fig. 4 is a snapshot of the CNN-BiLSTM data modeling breakdown in Python and Fig. 5 shows the flowchart which summarizes the overall modelling process for H_s forecasting.

2.7. Performance evaluation metrics

For model performance comparison in this study, eight evaluation metrics were used. Each metric (Eqs. 3–10) shows an aspect of performance evaluation demonstrating the accurateness of model performance in H_s forecasting for the study locations. Correlation coefficient (r) provides a value for strength in a two way linear association between the observed and predicted values (Mukaka, 2012). Willmott's Index of agreement (d) is a normalized dimensionless metric which measures accuracy and precision using squared residuals (Willmott et al., 2012). Nash Sutcliffe efficiency (NS) is a normalized statistic which measures the residual variance with measured data variance (McCuen et al., 2006). Legate and McCabe (Legates and McCabe, 2013) Index (LM) measures the divergence of a predictive model's performance. Average error and agreement measures based on sums of error magnitudes are considered superior to measures based on sums of squared errors (Willmott et al., 2015). The three performance measures complement each other and provide assurance of comprehensive evaluation of the predictive models used in this study. To further support the evaluation, computation of errors for the predictive models is also important (Raj et al., 2022). Root Mean Square Error (*RMSE*) and Mean Absolute Error (*MAE*) are widely used error metrics in predictive modelling (Chai and Draxler, 2014). *RMSE* computes the square root of the average of all measured differences between observed and predicted values. *RRMSE* is computed by dividing RMSE by the mean of the observed values. *MABE* is the average of all absolute errors from the difference in observed and predicted values. *MAPE* is the percentage form of the *MABE*.

1. Correlation Coefficient (r)

$$r = \left[\frac{\sum_{i=1}^{n}(DO_i - MDO)(DS_i - MDS)}{\sqrt{\sum_{i=1}^{n}(DO_i - MDO)^2 \sum_{i=1}^{n}(DS_i - MDS)^2}}\right]^2 \quad (3)$$

2. Willmott's Index of Agreement (d)

$$d = 1 - \left[\frac{\sum_{i=1}^{n}(DO_i - DS_i)^2}{\sum_{i=1}^{n}(|DS_i - MDO| + |DO_i - MDS|)^2}\right] \quad (4)$$

3. Nash-Sutcliffe Coefficient (NS)

$$NS = 1 - \left[\frac{\sum_{i=1}^{n}(DO_i - DS_i)^2}{\sum_{i=1}^{n}(DO_i - MDO)^2}\right], \ -\infty \le NS \le 1 \quad (5)$$

4. Legates and McCabe's Index (LM)

$$LM = 1 - \left[\frac{\sum_{i=1}^{n}|(DS_i - DO_i)|}{\sum_{i=1}^{n}|DO_i - MDS|}\right], \ 0 \le L \le 1 \quad (6)$$

5. Root Mean Square Error ($RMSE$)

$$RMSE = \sqrt{\left(\frac{1}{n}\right)\sum_{i=1}^{n}(DS_i - DO_i)^2} \quad (7)$$

6. Mean Absolute Error ($MABE$)

$$MABE = \frac{1}{n}\sum_{i=1}^{n}|(DS_i - DO_i)| \quad (8)$$

7. Relative Root Mean Square Error ($RRMSE$)

$$RRMSE = \frac{\sqrt{\left(\frac{1}{n}\right)\sum_{i=1}^{n}(DS_i - DO_i)^2}}{\frac{1}{n}\sum_{i=1}^{n}DO_i} \times 100 \quad (9)$$

8. Mean Absolute Percentage Error ($MAPE$)

$$\boldsymbol{MAPE} = \frac{1}{\mathrm{N}}\left(\sum_{N}^{i=1}\left|\frac{(DS_i - DO_i)}{DO_i}\right|\right) \times 100 \quad (10)$$

3. Results and discussion

This study used statistical evaluation on performance of models and the prediction errors to reveal the effectiveness of a new DL hybrid MVMD-CNN-BiLSTM model to accurately forecast H_s at Emu Park and Townville in Queensland in comparison to the benchmark AI models MVMD-MLP, MVMD-RF, MVMD MVMD-CB. The model with highest performance metrics (r, d, NS and LM) and lowest error metrics (RMSE,

Table 7
The model performance metrics for Townsville.

Model	Correlation Coefficient (r)	Willmott's Index of agreement (d)	Nash–Sutcliffe' Coefficient (NS)	Legates and McCabes' index (LM)
MVMD-RF	0.9936	0.9923	0.9872	0.9051
MVMD-MLP	0.9885	0.9861	0.9770	0.8732
MVMD-CatBoost	0.9979	0.9974	0.9957	0.9506
MVMD-CNN-BiLSTM	0.9986	0.9982	0.9970	0.9536

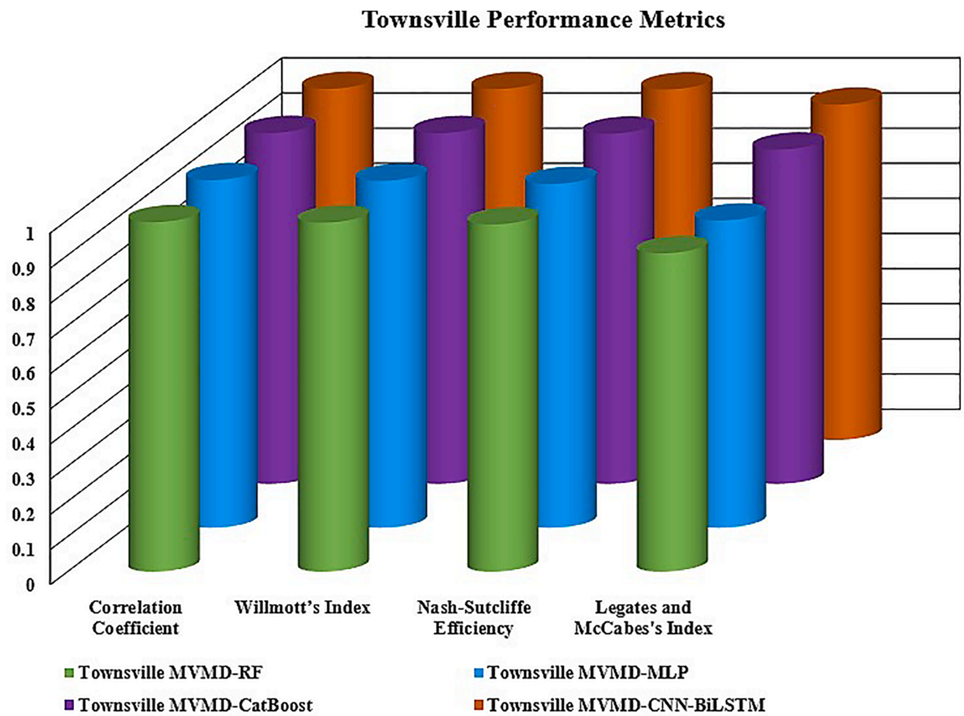

Fig. 6. Performance metrics comparison for Townsville.

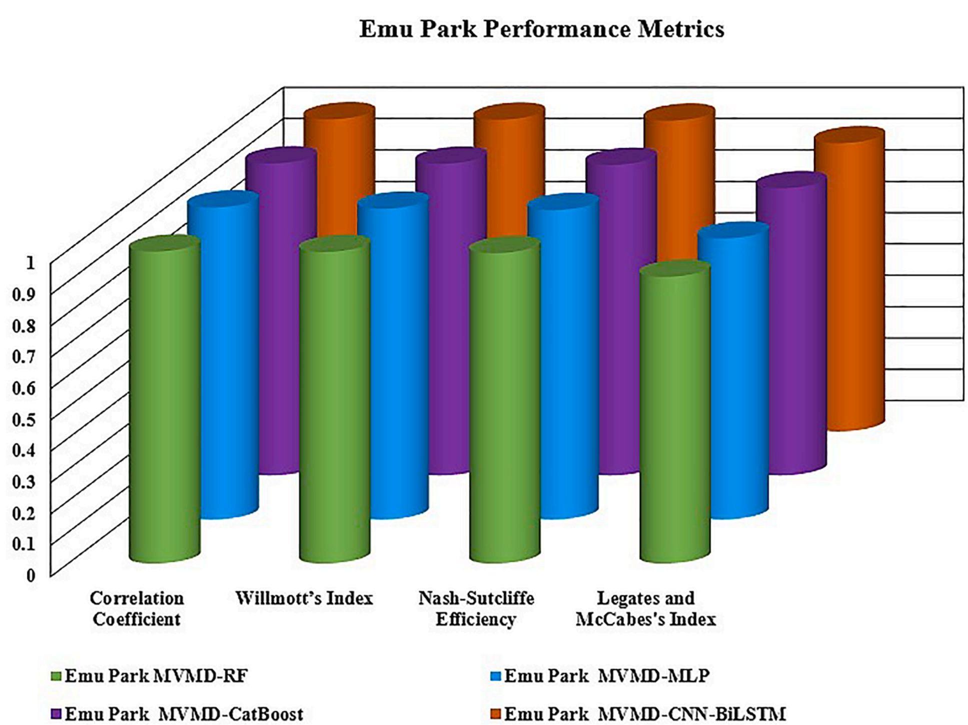

Fig. 7. Performance metrics comparison for Emu Park.

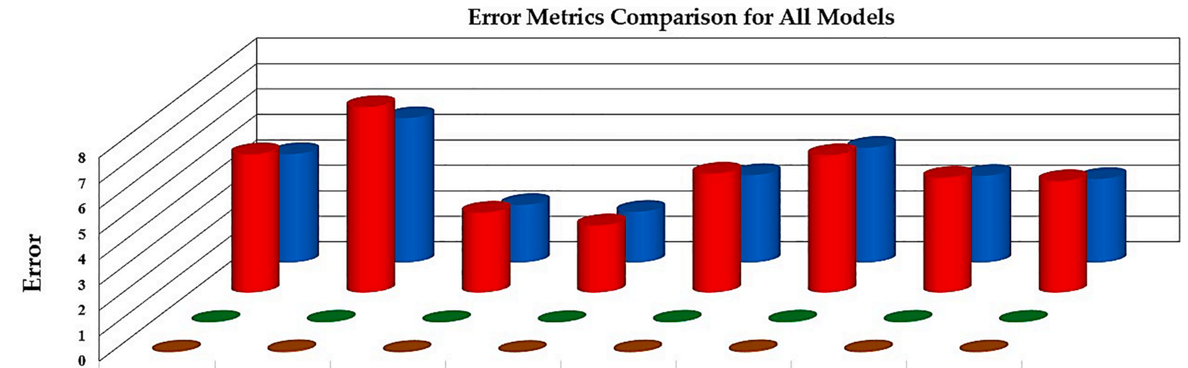

	Townsville MVMD-RF	Townsville MVMD-MLP	Townsville MVMD-CatBoost	Townsville MVMD-CNN-BiLSTM	Emu Park MVMD-RF	Emu Park MVMD-MLP	Emu Park MVMD-CatBoost	Emu Park MVMD-CNN-BiLSTM
RMSE	0.04	0.05	0.02	0.02	0.04	0.05	0.04	0.04
MABE	0.02	0.03	0.01	0.01	0.03	0.04	0.03	0.03
RRMSE	5.43	7.28	3.13	2.63	4.67	5.39	4.51	4.37
MAPE	4.26	5.67	2.26	1.99	3.43	4.51	3.40	3.28

Fig. 8. Error metrics for Townsville and Emu Park.

MABE, RRMSE and MAPE) is considered as the best model for accurately forecasting the H_s.

3.1. Performance metrics

Tables 6 and 7 show the performance metrics for the objective model (MVMD-CNN-BiLSTM) and the three benchmark models (MVMD-MLP, MVMD-RF, MVMD MVMD-CB) based on the testing dataset (Figs. 6 and 7).

Based on the computation of correlation coefficient, Willmott index, Nash-Sutcliffe's coefficient and Legate and McCabe's index, the model performance of the two study locations are shown in Tables 6 and 7. High performance metrics (> 0.9) was obtained for all developed models. This shows that all evaluated models are reliable in forecasting H_s. Highest performance metrics for MVMD-CNN-BiLSTM model supports the superior capability of forecasting H_s in comparison to other benchmark models. The MVMD-CNN-BiLSTM model achieved the highest values of correlation at both locations with values of 0.9957 and 0.9986 for Emu Park and Townsville, respectively. The MVMD-CNN-BiLSTM model also attained the highest values for Willmott Index (0.9946), Nash-Sutcliffe index (0.9914) and Legate and McCabe's index (0.919586) for Emu Park. Townsville also attained slightly better results for MVMD-CNN-BiLSTM with Willmott Index (0.9982), Nash-Sutcliffe index (0.9970) and Legate and McCabe's index (0.953560). Fig. 8 provides a graphical comparison of error metrics for all models. The error metrics also supports the superior performance of the MVMD-CNN-BiLSTM model with lower values of RMSE (0.0374), MABE (0.0272), RRMSE (4.371), MAPE (3.280) for Emu Park and RMSE (0.0170), MABE (0.012), RRMSE (2.6329), MAPE (1.991) for Townsville. The superior performance of all developed models is attributed to the data decomposition and optimization of hyperparameters of the model architecture. Superior performance of a hybrid MVMD model for forecasting daily H_s and daily wave energy in Queensland, Australia has also been demonstrated by Zheng et al. (2023) and Jamei et al. (2022) respectively. These two studies also verified the best performance of the examined respective objective hybrid MVMD models *via* Correlation, Willmott's Index of

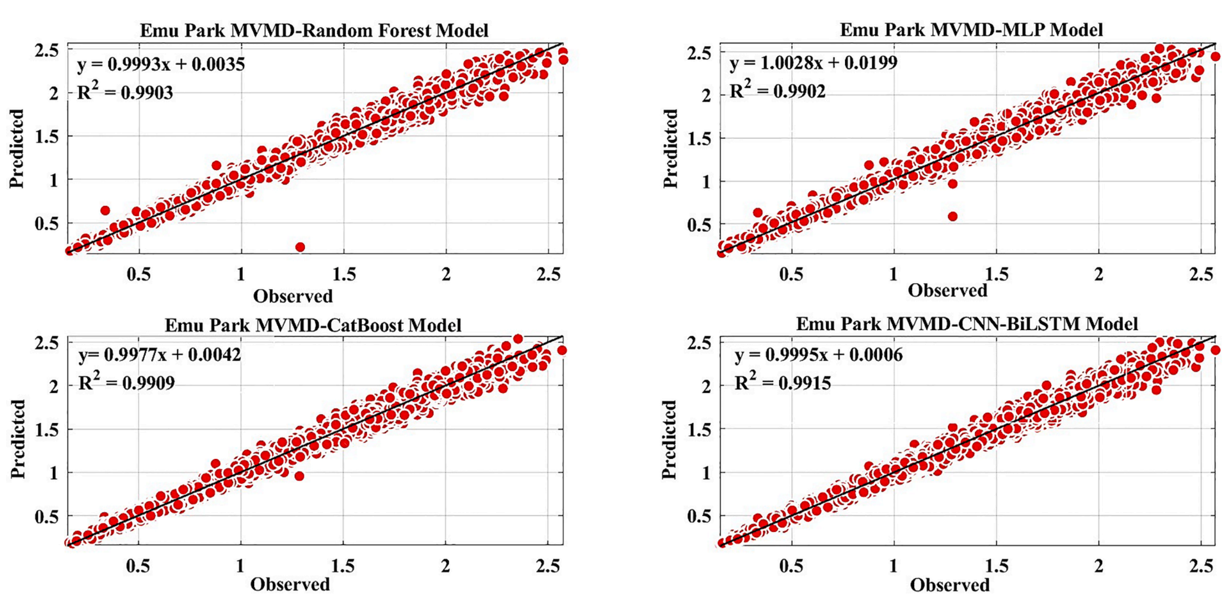

Fig. 9. Scatterplot for Emu Park.

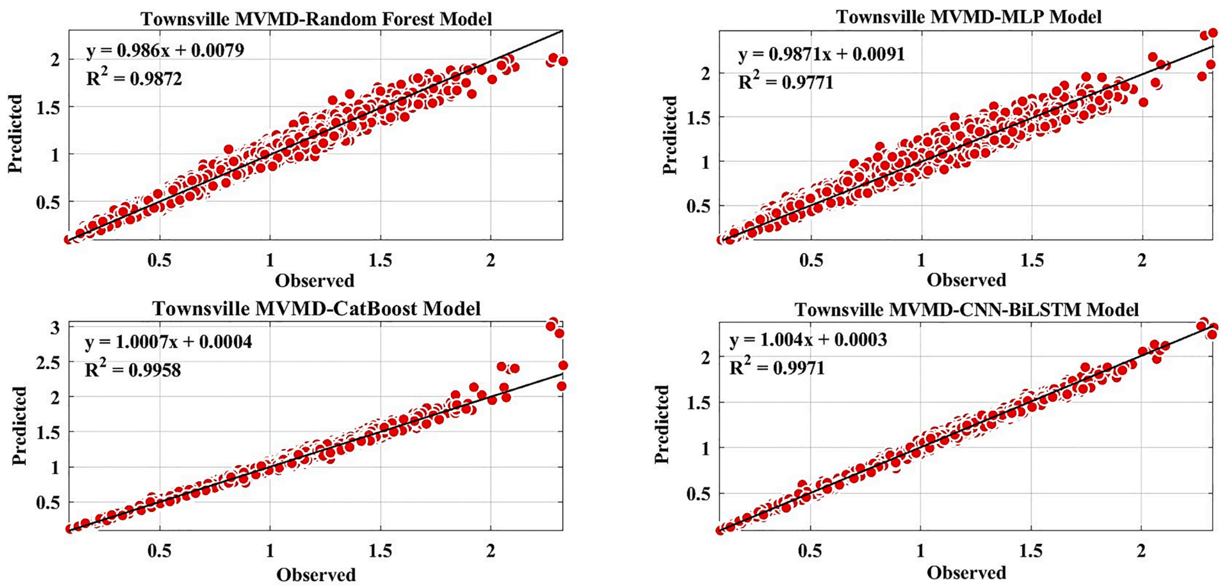

Fig. 10. Scatterplot for Townsville.

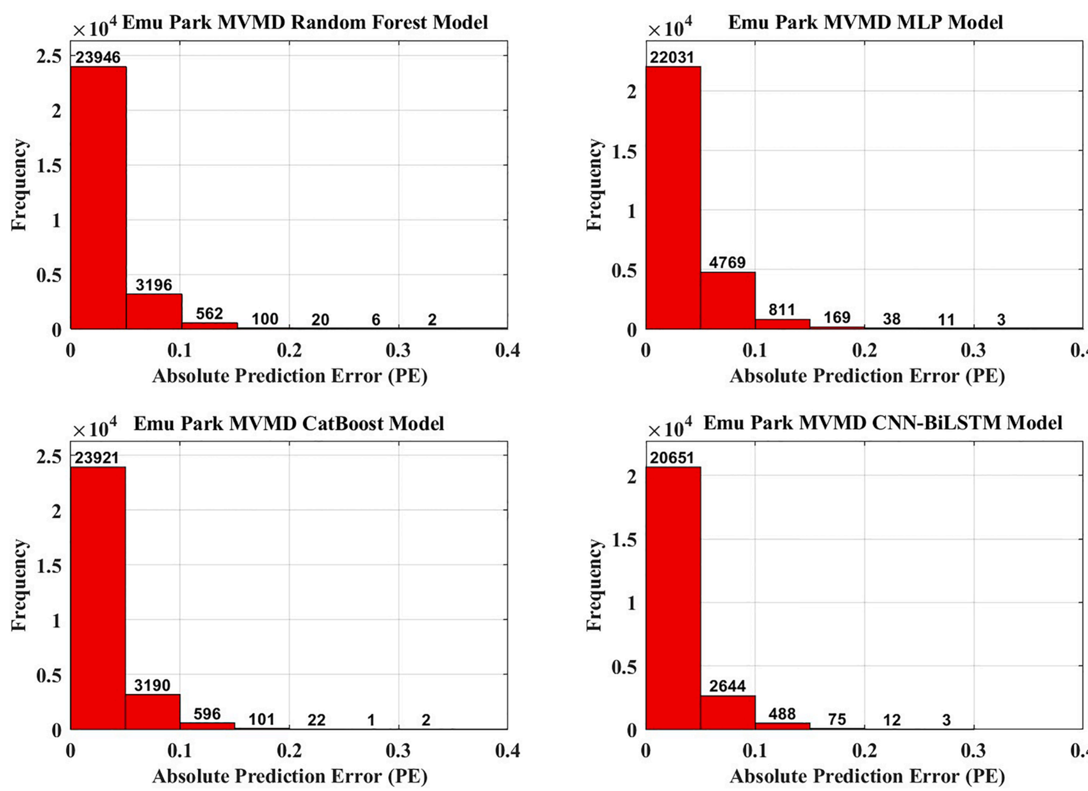

Fig. 11. Absolute prediction error histogram for Emu Park.

agreement, Nash–Sutcliffe' Coefficient, Legates and MacCabe's index, RRMSE and MAPE. Superior H_s forecasting quality of a new hybrid model a novel hybrid model called STL–CNN–PE was also demonstrated by highest correlation coefficient and lowest RMSE and MABE (Yang et al., 2021). The three performance metrics were also used to analyze the quantitative accuracy of models for forecasting of wave power density in China Sea (Zheng et al., 2016) and wave data stimulations in North Indian Ocean (Zheng and Song, 2021).

3.2. *Observed versus predicted data*

The scatterplots in Figs. 9 and 10 show the relationship between the observed and predicted H_s data. All models show points clustered together around the line of best fit with R^2 value > 0.9 for both Emu Park and Townsville. The closely packed cluster of points indicate the accuracy of the models. For predictions at both sites, MVMD-CatBoost also shows good performance when compared to MVMD-MLP and MVMD-Random Forest models. Highest R^2 values of MVMD-CNN-BiLSTM for Emu Park ($R^2 = 0.9915$) and Townville ($R^2 = 0.9971$) display greater

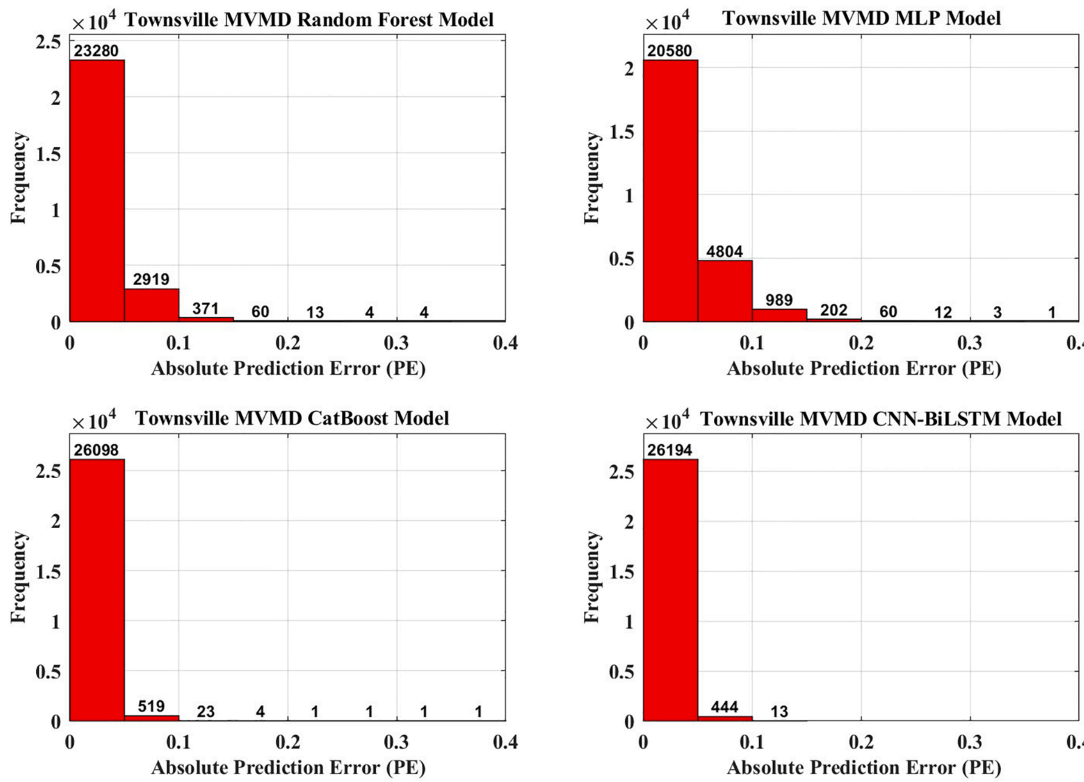

Fig. 12. Absolute prediction error histogram for Townsville.

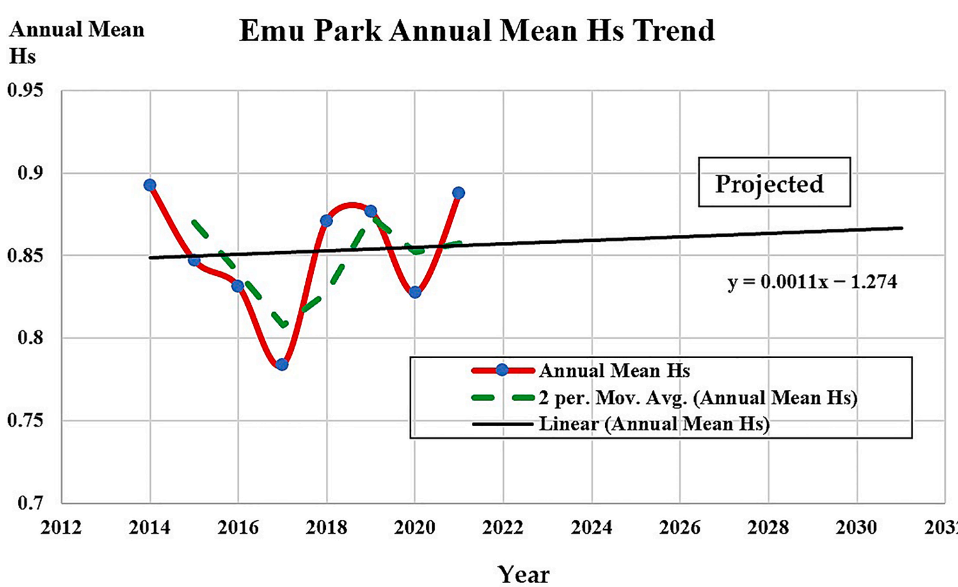

Fig. 13. Annual mean H_s linear projection for Emu Park.

accuracy of H_s prediction in comparison to other models. H_s forecasting precision of hybrid DL models was also demonstrated *via* scatter plots by Yang et al. (2021).

Figs. 11 and 12 are histograms of absolute prediction error (PE) for all models. The bins hold the frequency of absolute PE errors for both study sites. All models have higher frequency for lower values in the constructed histograms. Higher cluster of lower end values of prediction error indicates the higher accuracy of the model to predict the significant wave height (H_s). It is seen that CNN-BiLSTM have less values on the higher range of the histogram. Comparatively, MLP shows more PE values on the higher range at both study sites. The calculation and visualization of absolute prediction error confirms the accuracy of the models found through the scatterplots.

3.3. Trend analysis and linear projection

Figs. 13 and 14 provide annual mean H_s trend with a linear projection. The annual mean H_s for Emu Park and Townsville remains within the range of 0.78 to 0.9 and 0.62 to 0.69, respectively. The projected mean H_s values for Emu Park and Townsville are about 0.865 and 0.665 m, respectively, by the year 2031. This increase in H_s is consecutive to expected sea level rise of 0.2 m by 2030 in the Queensland region (Wang

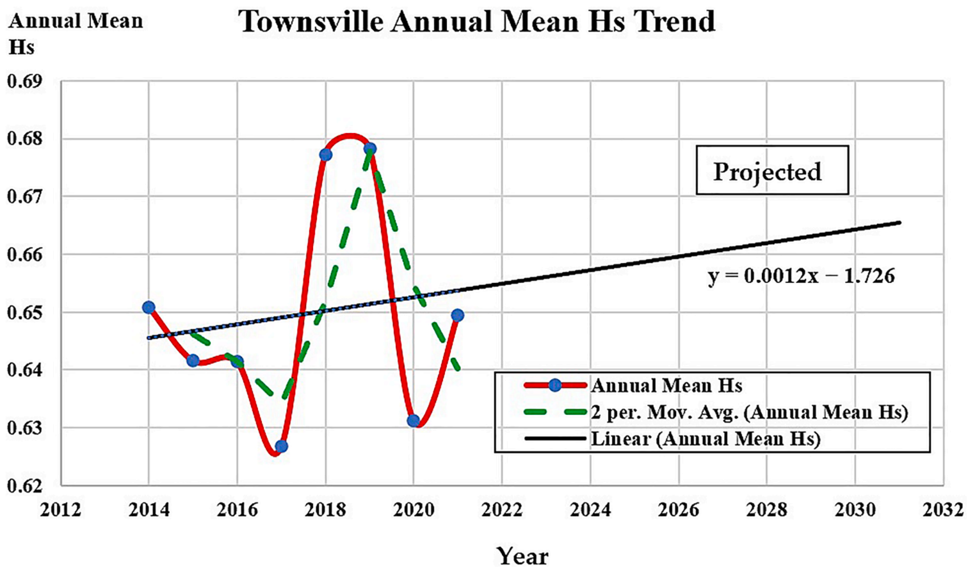

Fig. 14. Annual mean H_s linear projection for Townsville.

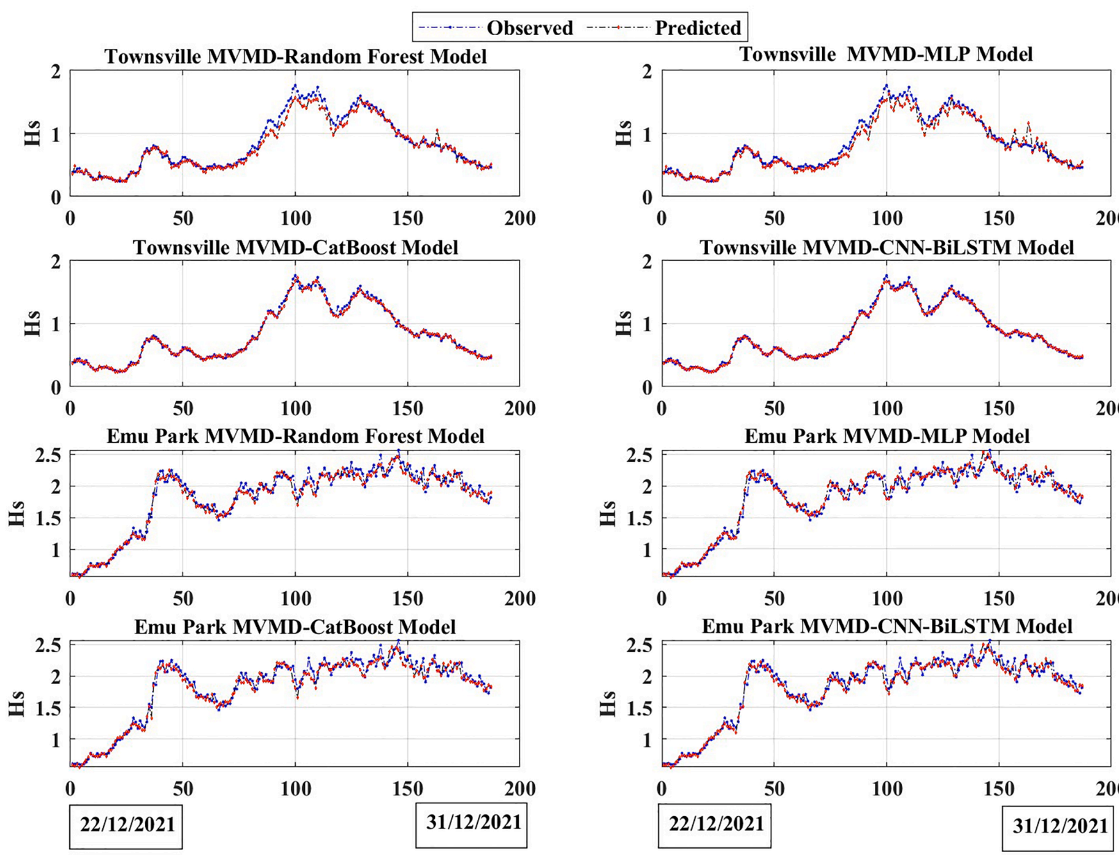

Fig. 15. Time series comparison of observed and predicted H_s for all models at both study sites.

et al., 2010). The combination of water depth increases and coastal inundation following sea level rise strongly influences the H_s, causing wave heights to increase significantly in deep-water areas (Shen et al., 2019). Sea level rise venture into increased wave power globally (Reguero et al., 2019). Wave energy is a function of significant wave height squared. Hence, Hs is an important factor for the wave energy and wave power generation. The wave energy is calculated as follows (Caloiero et al., 2020):

$$E = \frac{\rho g}{16}(\mathrm{H_s})^2 \tag{11}$$

where, $\boldsymbol{E}$ is energy, $\boldsymbol{\rho}$ is water density, $\boldsymbol{g}$ is gravity and $\mathbf{H_s}$ is significant wave height.

The wave power which is valid for all water conditions is as follows (Caloiero et al., 2020):

$$P = Ec_g \tag{12}$$

where, c_g is the group velocity of the wave.

Therefore, small increases in H_s result into big increases in wave energy output (Reikard et al., 2015). In this respect, Emu Park shows greater potential of higher wave energy influx for power generation. Linear projections of H_s also indicate an increase in ocean surface wind energy and warming at the two sites as wind energy and surface temperatures are the primary drivers of wave height (Reguero et al., 2019). There is a future scope of predicting teleconnection patterns using the hybrid models at the two sites. A study by Chen et al. (2023) states the importance of sustained density of significant wave height for a long period of time as a vital feature rather than isolated large heights for wave energy use.

For visualization of H_s on the testing phase for the two sites, Fig. 15 below shows the time series comparison of observed and predicted data points. All models provide close tracking of the observed data points supporting good model performances. The small spikes and fluctuations displayed by all models against H_s at both sites indicates the stability and reliability in prediction. Time series comparisons were also used by Zheng et al. (2023) and Yang et al. (2021) to show superior performance of a hybrid DL model. Zheng et al. (2016) also showed the visual accuracy of predicted data on wave power density using time series comparison. The important aspect presented in this study is the use of data decomposition with a new hybrid CNN-BiLSTM model which has not been studied in any past study for the two study sites. Given infrastructure for energy projects are extremely expensive and need accurate predictions showing stability in wave energy, such reliable predictions are needed for future wave energy projects. Furthermore, adding data decomposition technique to the AI modelling effectively show the improvement in accuracy for predictions (Eriksen and Rehman, 2023; Zheng et al., 2023). This is due to its ability to extract underlying features within the wave signal as intrinsic mode functions which are then used as predictor inputs for the target variable (H_s). This is the basis of the scientific background used in this study where signal decomposition, convolutional based neural network and two-way information processing long short-term memory AI architecture are combined for H_s prediction.

4. Conclusion

This study developed and validated an accurate and reliable hybrid MVMD-CNN-BiLSTM deep learning model for significant wave height prediction for two sites in Australia, Emu Park and Townsville. All models show high performance in terms of metrics such as correlation coefficient, Willmott index, Nash-Sutcliffe's coefficient and Legate and McCabe's index. The study also shows the importance of utilizing a data decomposition method for extraction of significant features from wave signals. The results confirm that the developed hybrid model can provide valuable insight into accurately forecasting wave height for consideration of wave power infrastructure installation which requires careful planning. The annual mean H_s trend analysis shows Emu Park has greater potential for sustainable ocean wave energy generation. The study can be extended to other parts of Australia to assess and predict significant wave height for potential wave energy resources.

CRediT authorship contribution statement

Nawin Raj: Conceptualization, Data curation, Formal analysis, Methodology, Resources, Investigation, Software, Validation, Visualization, Writing – original draft, Writing – review & editing. **Reema Prakash:** Writing – original draft, Writing – review & editing.

Declaration of competing interest

The authors declare that they have no known competing financial interests or personal relationships that could have appeared to influence the work reported in this paper.

Acknowledgments

None.

References

Ahmed, A.M., Deo, R.C., Feng, Q., Ghahramani, A., Raj, N., Yin, Z., Yang, L., 2021a. Hybrid deep learning method for a week-ahead evapotranspiration forecasting. Stoch. Environ. Res. Risk Assess. 1–19.

Ahmed, A.M., Deo, R.C., Ghahramani, A., Feng, Q., Raj, N., Yin, Z., Yang, L., 2022. New double decomposition deep learning methods for river water level forecasting. Sci. Total Environ. 831, 154722.

Ahmed, A.M., Deo, R.C., Raj, N., Ghahramani, A., Feng, Q., Yin, Z., Yang, L., 2021b. Deep learning forecasts of soil moisture: convolutional neural network and gated recurrent unit models coupled with satellite-derived MODIS, observations and synoptic-scale climate index data. Remote Sens. 13, 554 (Basel).

Aslan, M.F., Unlersen, M.F., Sabanci, K., Durdu, A., 2021. CNN-based transfer learning–BiLSTM network: a novel approach for COVID-19 infection detection. Appl. Soft. Comput. 98, 106912.

Breiman, L., 2001. Random forests. Mach. Learn. 45, 5–32.

Brink, H., Richards, J., Fetherolf, M., 2016. Real-World Machine Learning. Simon and Schuster.

Caloiero, T., Aristodemo, F., Ferraro, D.A., 2020. Changes of significant wave height, energy period and wave power in italy in the period 1979–2018. Environ. Sci. Proc. 2, 3.

Caloiero, T., Aristodemo, F., Ferraro, D.A., 2022. Annual and seasonal trend detection of significant wave height, energy period and wave power in the Mediterranean Sea. Ocean Eng. 243, 110322.

Chai, T., Draxler, R.R., 2014. Root mean square error (RMSE) or mean absolute error (MAE). Geosci. Model Dev. Discuss. 7, 1525–1534.

Chen, Y., Zhang, D., Li, X., Peng, Y., Wu, C., Pu, H., Zhou, D., Cao, Y., Zhang, J., 2023. Significant wave height prediction through artificial intelligent mode decomposition for wave energy management. Energy AI 14, 100257.

Chua, L.O., Roska, T., 1993. The CNN paradigm. IEEE Trans. Circuits Syst. I Fundam. Theory Appl. 40, 147–156.

Deka, P.C., Prahlada, R., 2012. Discrete wavelet neural network approach in significant wave height forecasting for multistep lead time. Ocean Eng. 43, 32–42.

Deo, M., Gondane, D., Sanil Kumar, V., 2002. Analysis of wave directional spreading using neural networks. J. Waterw. Port. Coast. Ocean. Eng. 128, 30–37.

Eriksen, T., Rehman, N.u., 2023. Data-driven nonstationary signal decomposition approaches: a comparative analysis. Sci. Rep. 13, 1798.

Feng, Z., Hu, P., Li, S., Mo, D., 2022. Prediction of significant wave height in offshore china based on the machine learning method. J. Mar. Sci. Eng. 10, 836.

Gardner, M.W., Dorling, S., 1998. Artificial neural networks (the multilayer perceptron)—A review of applications in the atmospheric sciences. Atmos. Environ. 32, 2627–2636.

Guillou, N., Chapalain, G., 2020. Assessment of wave power variability and exploitation with a long-term hindcast database. Renew. Energy 154, 1272–1282.

Hancock, J.T., Khoshgoftaar, T.M., 2020. CatBoost for big data: an interdisciplinary review. J. Big Data 7, 1–45.

Huang, G., Wu, L., Ma, X., Zhang, W., Fan, J., Yu, X., Zeng, W., Zhou, H., 2019. Evaluation of CatBoost method for prediction of reference evapotranspiration in humid regions. J. Hydrol. 574, 1029–1041 (Amst).

Hughes, M.G., Heap, A.D., 2010. National-scale wave energy resource assessment for Australia. Renew. Energy 35, 1783–1791.

Jain, P., Deo, M., Latha, G., Rajendran, V., 2011. Real time wave forecasting using wind time history and numerical model. Ocean. Model. 36, 26–39 (Oxf).

Jamei, M., Ali, M., Karbasi, M., Xiang, Y., Ahmadianfar, I., Yaseen, Z.M., 2022. Designing a multi-stage expert system for daily ocean wave energy forecasting: a multivariate data decomposition-based approach. Appl. Energy 326, 119925.

Karbasi, M., Jamei, M., Ali, M., Abdulla, S., Chu, X., Yaseen, Z.M., 2022. Developing a novel hybrid auto encoder decoder bidirectional gated recurrent unit model enhanced with empirical wavelet transform and Boruta-Catboost to forecast significant wave height. J. Clean. Prod. 379, 134820.

Kwiatkowski, D., Phillips, P.C., Schmidt, P., Shin, Y., 1992. Testing the null hypothesis of stationarity against the alternative of a unit root: how sure are we that economic time series have a unit root? J. Econom. 54, 159–178.

Legates, D.R., McCabe, G.J., 2013. A refined index of model performance: a rejoinder. Int. J. Climatol. 33, 1053–1056.

López, I., Andreu, J., Ceballos, S., De Alegría, I.M., Kortabarria, I., 2013. Review of wave energy technologies and the necessary power-equipment. Renew. Sustain. Energy Rev. 27, 413–434.

Lopez, J.H., 1997. The power of the ADF test. Econ. Lett. 57, 5–10.

Manuca, R., Savit, R., 1996. Stationarity and nonstationarity in time series analysis. Phys. D Nonlinear Phenom. 99, 134–161.

McCuen, R.H., Knight, Z., Cutter, A.G., 2006. Evaluation of the Nash–Sutcliffe efficiency index. J. Hydrol. Eng. 11, 597–602.

Mukaka, M.M., 2012. A guide to appropriate use of correlation coefficient in medical research. Malawi Med. J. 24, 69–71.

Nason, G.P., 2006. Stationary and non-stationary time series. Stat. Volcanol. 60.

Prokhorenkova, L., Gusev, G., Vorobev, A., Dorogush, A.V., Gulin, A., 2018. CatBoost: unbiased boosting with categorical features. Adv. Neural Inf. Process. Syst. 31.
Raj, N., Brown, J., 2021. An EEMD-BiLSTM algorithm integrated with Boruta random forest optimiser for significant wave height forecasting along coastal areas of Queensland, Australia. Remote Sens. 13, 1456.
Raj, N., Gharineiat, Z., Ahmed, A.A.M., Stepanyants, Y., 2022. Assessment and prediction of sea level trend in the South Pacific Region. Remote Sens. 14, 986 (Basel).
Reguero, B.G., Losada, I.J., Méndez, F.J., 2019. A recent increase in global wave power as a consequence of oceanic warming. Nat. Commun. 10, 205.
Reikard, G., Robertson, B., Buckham, B., Bidlot, J.-R., Hiles, C., 2015. Simulating and forecasting ocean wave energy in western Canada. Ocean Eng. 103, 223–236.
Ribal, A., Young, I.R., 2019. 33 years of globally calibrated wave height and wind speed data based on altimeter observations. Sci. Data 6, 1–15.
Segal, M.R., 2004. Machine learning benchmarks and random forest regression.
Sharma, E., Deo, R.C., Soar, J., Prasad, R., Parisi, A.V., Raj, N., 2022. Novel hybrid deep learning model for satellite based PM10 forecasting in the most polluted Australian hotspots. Atmos. Environ. 279, 119111.
Shen, Y., Deng, G., Xu, Z., Tang, J., 2019. Effects of sea level rise on storm surge and waves within the Yangtze River Estuary. Front. Earth Sci. 13, 303–316.
Song, T., Wang, J., Huo, J., Wei, W., Han, R., Xu, D., Meng, F., 2023. Prediction of significant wave height based on EEMD and deep learning. Front. Mar. Sci. 10, 1089357.
ur Rehman, N., Aftab, H., 2019. Multivariate variational mode decomposition. IEEE Trans. Signal Process. 67, 6039–6052.
Vanem, E., 2016. Joint statistical models for significant wave height and wave period in a changing climate. Mar. Struct. 49, 180–205.
Veerabhadrappa, K., Suhas, B., Mangrulkar, C.K., Kumar, R.S., Mudakappanavar, V., Seetharamu, K., 2022. Power generation using ocean waves: a review. Global Trans. Proc. 3, 359–370.
Wang, X., Stafford, S.M., McAllister, R.R.J., Leitch, A., McFallan, S., Meharg, S., 2010. Coastal inundation under climate change: a case study in South East Queensland, CSIRO Climate Adaptation Flagship Working paper No. 6.
Willmott, C.J., Robeson, S.M., Matsuura, K., 2012. A refined index of model performance. Int. J. Climatol. 32, 2088–2094.
Willmott, C.J., Robeson, S.M., Matsuura, K., Ficklin, D.L., 2015. Assessment of three dimensionless measures of model performance. Environ. Model. Softw. 73, 167–174.
Wimalaratna, Y.P., Hassan, A., Afrouzi, H.N., Mehranzamir, K., Ahmed, J., Siddique, B. M., Liew, S.C., 2022. Comprehensive review on the feasibility of developing wave energy as a renewable energy resource in Australia. Clean. Energy Syst., 100021
Yang, S., Deng, Z., Li, X., Zheng, C., Xi, L., Zhuang, J., Zhang, Z., Zhang, Z., 2021. A novel hybrid model based on STL decomposition and one-dimensional convolutional neural networks with positional encoding for significant wave height forecast. Renew. Energy 173, 531–543.
Zhang, S., Li, C.M., Ye, W., 2021. Damage localization in plate-like structures using time-varying feature and one-dimensional convolutional neural network. Mech. Syst. Signal Process. 147, 107107.
Zhang, Y., Zhao, Z., Zheng, J., 2020. CatBoost: a new approach for estimating daily reference crop evapotranspiration in arid and semi-arid regions of Northern China. J. Hydrol. 588, 125087 (Amst).
Zhao, L., Li, Z., Zhang, J., Teng, B., 2023. An integrated complete ensemble empirical mode decomposition with adaptive noise to optimize LSTM for significant wave height forecasting. J. Mar. Sci. Eng. 11, 435.
Zheng, C., Song, H., 2021. Case study of a short-term wave energy forecasting scheme: North Indian Ocean. J. Ocean Univ. China 20, 463–477.
Zheng, C.W., Li, C.Y., Chen, X., Pan, J., 2016. Numerical forecasting experiment of the wave energy resource in the China Sea. Adv. Meteorol. 2016, 5692431.
Zheng, Z., Ali, M., Jamei, M., Xiang, Y., Abdulla, S., Yaseen, Z.M., Farooque, A.A., 2023. Multivariate data decomposition based deep learning approach to forecast one-day ahead significant wave height for ocean energy generation. Renew. Sustain. Energy Rev. 185, 113645.
Zhou, S., Bethel, B.J., Sun, W., Zhao, Y., Xie, W., Dong, C., 2021. Improving significant wave height forecasts using a joint empirical mode decomposition–long short-term memory network. J. Mar. Sci. Eng. 9, 744.